4th Conference on Sustainability in Civil Engineering (CSCE'22)
Department of Civil Engineering
Capital University of Science and Technology, Islamabad Pakistan

3D FINITE ELEMENT ANALYSIS OF REINFORCED CONCRETE BEAMS UNDER FIRE

[a] Javaria Mehwish*, [b] Katherine Cashell, [c] Rabee Shamass

a: Civil & Environmental Engineering, Brunel University London, javaria.mehwish@brunel.ac.uk
b: Civil & Environmental Engineering, Brunel University London, Katherine.cashell@brunel.ac.uk
c: Civil & Environmental Engineering, London South Bank University, shamassR@Lsbu.ac.uk
* PhD Candidate Brunel University London

Abstract- This paper presents a numerical investigation of the fire behaviour of reinforced concrete beams reinforced with carbon steel. The main aim of this paper is to propose and validate a detailed finite-element model that considers the nonlinear behaviour of the materials and the heat transfer parameters that affect the fire performance of steel reinforced concrete beams using commercial FE software ABAQUS. The analysis was performed using sequentially coupled thermal stress analysis, for which the thermal analysis was firstly performed, and the structural analysis was then conducted. The EC2 constitutive material models for concrete in tension and compression at elevated temperature were simulated while the steel was modelled using either elastic-perfectly plastic or with strain hardening suggested in the EC2. Regarding the heat transfer, models with and without radiation heat transfer were conducted. The numerical results were compared with three tested beams. It was found that numerical models without radiation heat transfer provided results in good agreement with the test results. The elastic-perfect plastic material model for steel rebar at elevated temperatures can be utilized in FEA to reduce the computational time. However, the steel model with strain hardening provided more accurate predictions.

Keywords- Abaqus, fire analysis, material modelling and reinforced concrete.

1. Introduction

This paper is concerned with the elevated temperature behaviour of reinforced concrete beams. Reinforced concrete (RC) is one of the most commonly used structural materials and is regularly employed for various structures, including office blocks, hospitals, schools, and bridges. In addition to efficiently using the constituent materials, it behaves well in extreme conditions such as fire and offers excellent structural resistance. The fire resistance of a building or structural element is defined as the time in which the structural element retains sufficient structural integrity and stability. When a structural member is exposed to fire, it loses strength as the material properties deteriorate, increasing internal stress in the element. This may lead to the redistribution of stresses in the structure, loss of key elements and even possible collapse of the overall structure. Studies by Beitel and Iwankiw [1] and Lue Taerwe [2] assessed several reinforced concrete structures that suffered full or partial collapse due to fire, such as the warehouse building in Ghent, Belgium collapsed following a fire in 1974. According to statistics by N.N Brushlinsky [3], the average number of deaths caused by fire is 43,200 per year in 3.7 million fire incidents in 39 countries. The United Kingdom, on the other hand, faced 367 deaths per year [3] due to fire. In 2017, the recent fire incident in London Grenfell highlighted that this type of extreme event, although rare, is still a real threat to both structural integrity and human life.

Under a real fire scenario, the heat is transferred through convection, radiation and conduction. Radiation heat transfer mode should be considered when conduction and convection are small, or the-time scale is small for which conduction and convection effects are too slow, and radiation becomes the predominant transfer mode [4]. Conventionally heat analysis in RC members is performed through all three modes of heat transfer [5-7]. This subject is still not addressed in most research [15-16]. Therefore, in the current study finite element analysis (FEA) of RC beam is performed using

conduction and convection mode of heat transfer only. Thermo-structural analysis of the RC beam shows that this hypothesis produces very excellent results.

2. Finite element analysis

This section discusses the development of a three-dimensional finite element model that can simulate the nonlinear thermal and structural response of an RC beam under different fire conditions and employs a sequentially coupled analysis approach, including a thermal analysis to simulate the spread of elevated temperature through the section, followed by a Thermal stress analysis. Thermal stress analysis is performed in two models: (i) the heat transfer analysis model, and (ii) the structural model. The results of the first analysis model are used as a thermal load for the structural analysis model.

2.1. Thermal Analysis

A nonlinear transient heat transfer analysis (as the heat flow rate keeps changing with time and produces varying rates of heat transfer) is simulated in the first step to determine the thermal response of the RC beam and nodal temperature histories. In this analysis, the temperature field is calculated without consideration of the stress/deformation field. The result is then used as a thermal load for the structural analysis. Heat flux is the thermal energy flow inside the material per unit area per unit time is computed by Abaqus by defining fire load, convection, and conduction parameters.

The fire load determined from the standard fire time-temperature curve is applied in the form of amplitude on the external boundary of the model. Convection is modelled through surface film condition interaction as heat flow from surrounding is through the model surface. Film coefficient is the same as defined above and is used along with sink temperature as 1 with sink amplitude same as fire load. Conduction between two surfaces in one element, from concrete to steel rebars of the beam passes through embedded constraint in Abaqus. This is achieved when the steel rebar is fully embedded in the host region concrete.

The model is divided into a number of finite elements. The mesh for both thermal and structural models should be the same to make them compatible. Mesh sizes 50mm, 25mm and 10mm are used to study the effect of mesh size on the convergence time and results. A mesh size of 25mm has been used in the current study, providing more accurate results in a reasonable time. The three-dimensional eight-node solid liner heat transfer element (DC3D8) with a temperature degree of freedom was used to model the concrete beams for thermal analysis. Similarly, a two-node heat transfer link element (DC1D2) with a temperature degree of freedom is used for reinforcing steel.

The input parameters required in heat transfer analysis include fire load and thermal material properties. Three different forms of fire load, including fire curve ISO-834 [8], ASTM E119 [9] and short design fire (data is chosen from a practical test performed by Kodur [6], are selected for the present study.

Thermal material properties like thermal conductivity, specific heat capacity, thermal expansion, density, and temperature-dependent elasticity modulus are required in heat transfer analysis. All this data is available in Eurocode 2004 Part 1-2 (EC 2) [10], except the thermal expansion coefficient which is taken from ASCE manual 78 [11] and expressed in equations below. In EC 2[10] thermal elongation is given whereas input data required the thermal coefficient of material in Abaqus [4] therefore this value is taken from the ASCE [11] manual.

For siliceous and carbonate aggregate concrete

$$\alpha_c = (.008\theta + 12)\ 10^{-6} \text{ for } 20°C \le \theta \le 800°C \qquad (1)$$

Similarly, for steel following expression can be used.

$$\alpha_s = (.004\theta + 12)\ 10^{-6} \quad \text{for } \theta < 1000°C \qquad (2)$$

$$\alpha_s = 16 \text{ x} 10^{-6} \quad \text{for } \theta \ge 1000°C \qquad (3)$$

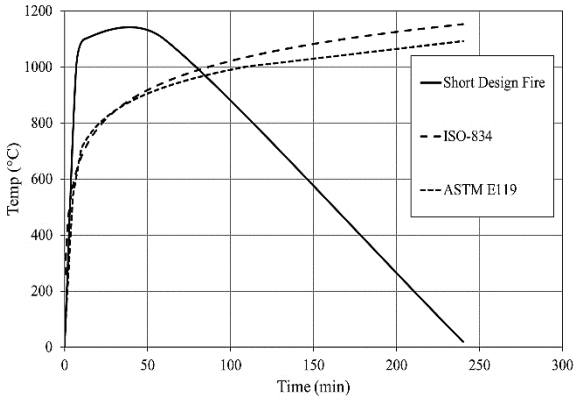

Figure 1. Time-dependent temperature curves. [6,8,9]

2.2. Thermal stress analysis

Structural analysis is performed in the second model using sequentially coupled thermal stress analysis. The second model uses the same heat transfer analysis model with further modification. In this model, concrete is discretized using eight-nodded continuum elements (C3D8) with three degrees of freedom; namely three translations in x, y, and z directions, as they are capable of accounting for cracking of concrete in tension, crushing of concrete in compression, creep, and large strain [4]. Steel reinforcement is defined using two-noded link truss elements (T3D2). As it is assumed to be deformed by axial stretching only. They are pin jointed at their nodes [4].

Thermal structural stress analysis is performed in two steps. In the first step, the mechanical load is applied along with boundary conditions per the test specimen. In the second step, thermal load from heat transfer analysis is applied through predefined fields. The implicit solver available in Abaqus/Standard based on an iteration process to enforce equilibrium conditions is utilised for analysis. No bond slip is considered between concrete and steel, and temperature is considered uniform through the full length of the beam.

3. Material Modelling

Mechanical material properties like compressive and tensile strength of the material are required in stress analysis. Constitutive material models for steel and concrete are chosen from EC 2 [10], which implicitly include concrete transient strain. Also, only normal strength concrete is considered, so thermal spalling is negligible. The concrete material model is defined under the concrete damage plasticity material model (CDP) [4]. The input parameters for CDP models are shown in Table 1.

Table 1. CDP Model input parameters

Dilatation angle ψ	Eccentricity ϵ	Fb0/fc0	K_c	Viscosity parameter
35	.1	1.16	.666667	.0003

The problems related to achieving the convergence of the solution, caused by the non-linearity of the material model, were solved by viscosity stabilization μ [12]. The selection of the viscosity parameter μ was made iteratively after analyzing its impact on the convergence results. Finally, a value of 0.0003 was used, and the analysis shows that it completed the convergence in a reasonable time.

3.1. Concrete under compression

The concrete damage plasticity model is implemented with concrete compression hardening, concrete tension stiffening, and the concrete compression damage parameter. These parameters are modelled with the temperature range. Concrete compression behaviour is defined through the stress-strain curve using a constitutive material model

from EC2 [10]. Concrete strain is divided into two parts. So total strain ε_t in the inelastic-cracking equals to cracking the strain ε_{cr} and elastic strain ε^{el} [4], it is explained in expression below.

$$\varepsilon_{cr} = \varepsilon_t - \varepsilon^{el} \quad (4)$$

Similarly, damage parameter d_c is defined as the ratio of the cracking strain to the total strain. The value of d_c is valid only for descending branch of the stress-strain curve. The following expression [4] is used to calculate the damage parameter.

$$d_c = \frac{f_{cm} - \sigma_c}{f_{cm}} \quad (5)$$

3.2. Concrete under Tension

The tensile strength of the concrete reduces at high temperatures and is also calculated from EC 2 [10]. There is a software limitation to utilize concrete tension damage parameters along with temperature range. So, crack propagation in concrete under tension is modelled through fracture energy.

The fracture energy of concrete GF [N/m], defined as the energy required to propagate a tensile crack of a unit area, should be determined by related tests. Without experimental data, GF in [N/m] for ordinary, normal-weight concrete can be estimated from the following equation from fib Model 2010[13]. Fracture energy calculated through this expression has been used in the present study with reduced compressive strength at the high-temperature range.

$$G_F = 73.f_{cm}{}^{.18} \quad (6)$$

f_{cm} is the mean compressive strength

.

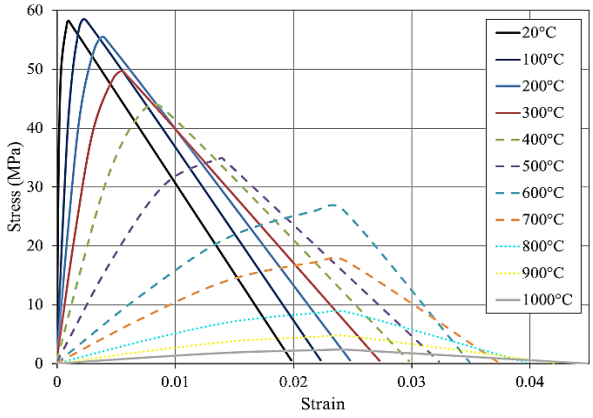

Figure 2. Stress-strain curves of concrete at elevated temperatures.

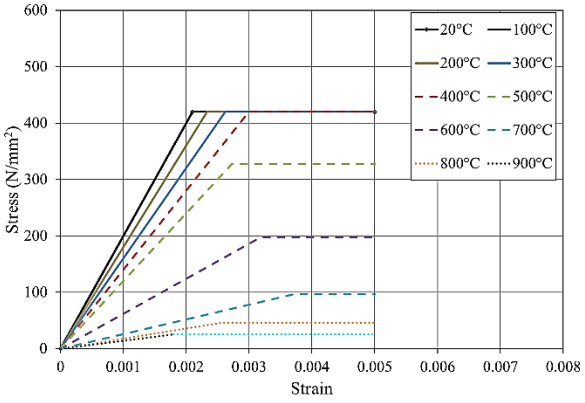

Figure 3. Perfect plastic material model for carbon steel at elevated temperatures.

3.3. Reinforcing Carbon Steel

Steel reinforcement can be modelled as perfectly plastic material with a single yield stress value per temperature [4]. In this material model, strain is increased elastically with increased stress, and once yield occurs, the material will deform plastically without increasing stress. Steel reinforcement is considered a perfectly plastic material and identical in tension and compression. The other option is miss yield surface to define isotropic yielding of steel reinforcement and defined by uniaxial yield surface against uniaxial plastic strain along with the temperature. The plastic material data should be Cauchy stress and logarithmic strain. Following equations are used for converting simple nominal stress–strain to true stress, and logarithmic plastic strain is as follows [4]. Both models are utilized in this study.

$$\sigma_{true} = \sigma_{nom} = (1 + \varepsilon_{nom}) \quad (7)$$

$$\varepsilon_{ln}^{pl} = ln(1 + \varepsilon_{nom}) - \frac{\sigma_{true}}{E} \quad (8)$$

The constitutive material models of steel from EC 2 [11] are utilized to define isotropic steel yielding. The proportional limit is the end of an elastic region on the stress-strain curve. This is given as a ratio to yield strength in EC 2 [11], whereas, in the present study, it is taken as constant at 0.2% strain. The results produced from FEA using the new proposed proportional limits are in excellent agreement with the test results.

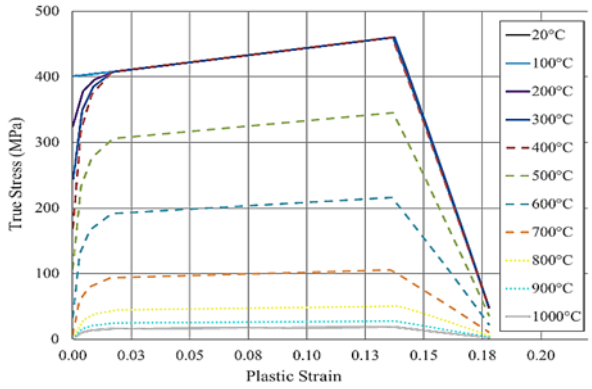

Figure 4. Stress-strain curve for carbon steel at elevated temperatures using EC 2 [10] material model.

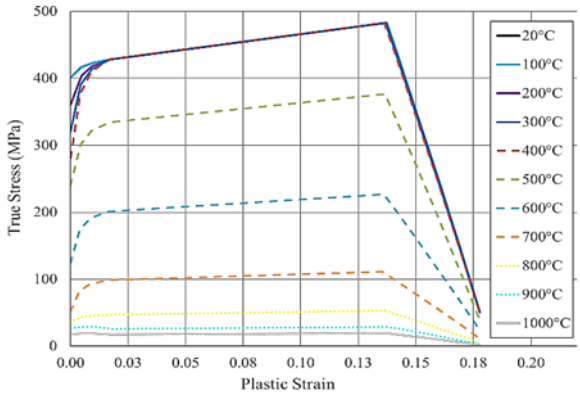

Figure 5. Stress-strain curve for carbon steel at elevated temperatures using EC 2 [10] material model considering 0.2% strain at the proportional limit

4. Validation

RC beams tested under fire by Wu [14] and Dwaikat and Kodur [6], respectively, are chosen in the present study to validate the proposed FEA. The results show the capability and accuracy of the current FE model. These tests were selected because their results were thorough enough to allow for FE simulations and comparisons. The layout and arrangement of tested beams are given in subsequent sections. General properties are provided below.

Table 2. General properties of the tested beams.

Study	Beam designation	Fire exposure	Support condition	Concrete strength fc (MPa)	Aggregate type	Steel strength fy (MPa)	Applied Load (KN)
W. H. Wu	Beam slab 1	ISO 834	SS	21	Carbonate	240	Distributed load
Dwaikat and Kodur	B1	ASTM E119	SS	58.2	Siliceous	420	50
	B2	SF	AR	58.2	Siliceous	420	50

Three different types of beams are selected for the validation purpose to see the effect of different type of concrete strength, steel strength, fire exposure and support condition. The beam tested by Wu [14] was simply supported and exposed to ISO-834 [8] fire with low-strength concrete and carbonation aggregates. Whereas two different beams were tested by Kodur [6]. They have similar material properties as given in Table 2, but different fire exposure was applied. The beam exposed to the ASTM E119 [9] curve was simply supported, whereas the other beam was axially restrained (AR) and exposed to short fire (SF).

4.1. Test by Wu et al.

The sample tested beam [14] was 5.1 m long in span, and 4.0 m of the internal span was exposed to fire, as shown in the figure below. An overlying slab of 80 mm thickness was placed on top of the beam during the fire test. An additional distributed load of 300 kg/m2 was applied on the top of the overlying slab, so the total load acting on the beam was a combination of distributed load and overlying slab load.

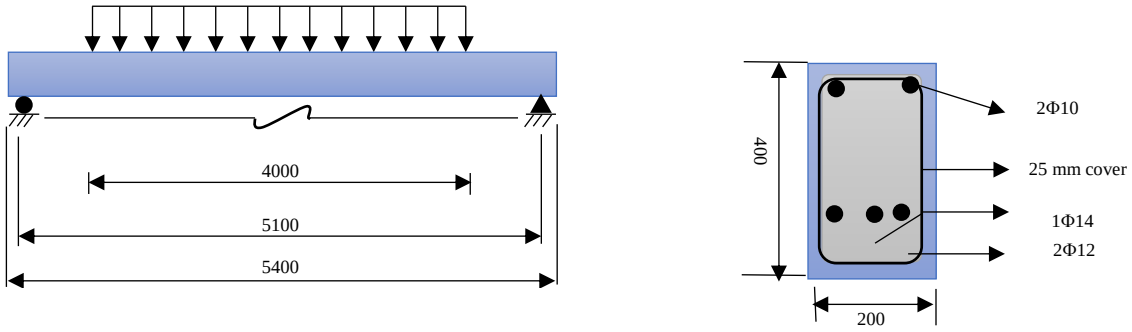

Figure 6 Test by Wu et al. [15]

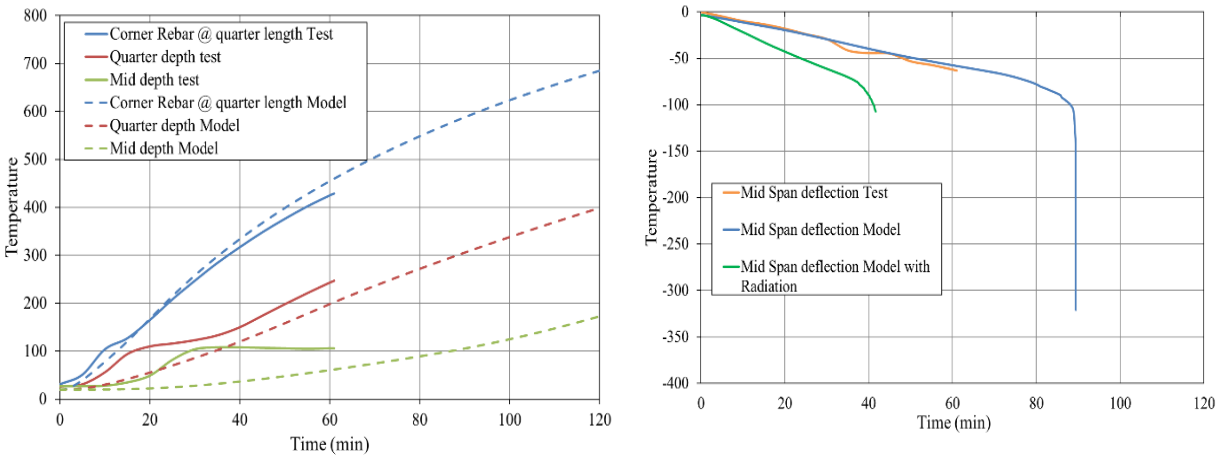

Figure 7. Comparison of predicted and measured rebar and concrete temperature and displacement.

Fire analysis of the sample beam was performed in Abaqus [4] using the abovementioned procedure. Heat transfer analysis was performed first considering radiation and then without it. Stress analysis results in figure (7) show that the FEA of the sample beam with radiation produced an early failure of the beam. In contrast, the model analyzed without radiation showed a closer deflection prediction with compression failure. The validity of the proposed methodology for heat transfer analysis is demonstrated by the close match between the FEA model and test outcomes.

4.2. Test by Kodur et al.

Two concrete beams named B-1 & B2 were tested under different fire exposure by Dwaikat and Kodur [6]. They are analyzed by applying the above numerical procedure to validate the proposed approach of heat transfer analysis without radiation and the new proposed steel material model. The arrangement of the two beams is the same, except the fire load was different. The general layout is shown in figure 8.

The authors applied force 30 minutes before the start of the fire and sustained it until no more deformation could be recorded in the fire tests. This was chosen as the initial condition for the beam's deflection. After that, the load was

kept constant for the duration of the fire exposure. B1 was exposed to ASTM E119 fire, and the short fire was applied to B2. Beam B1 failed to sustain load in fire after 180 mins. At the same time, B2 did not fail during fire exposure.

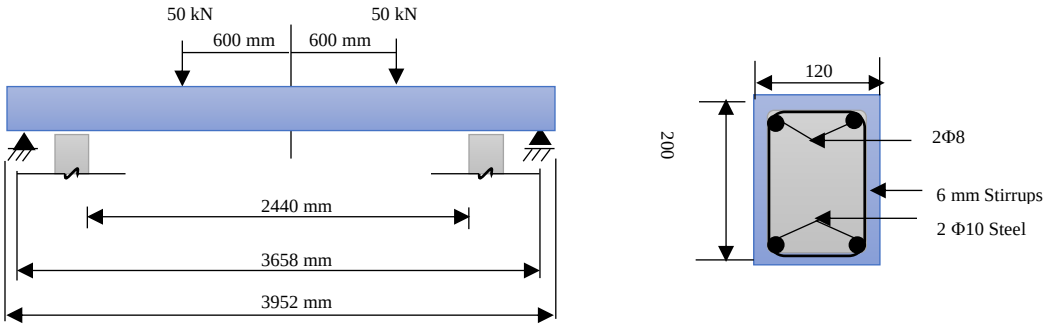

Figure 8. Test by Kodur et al. [6].

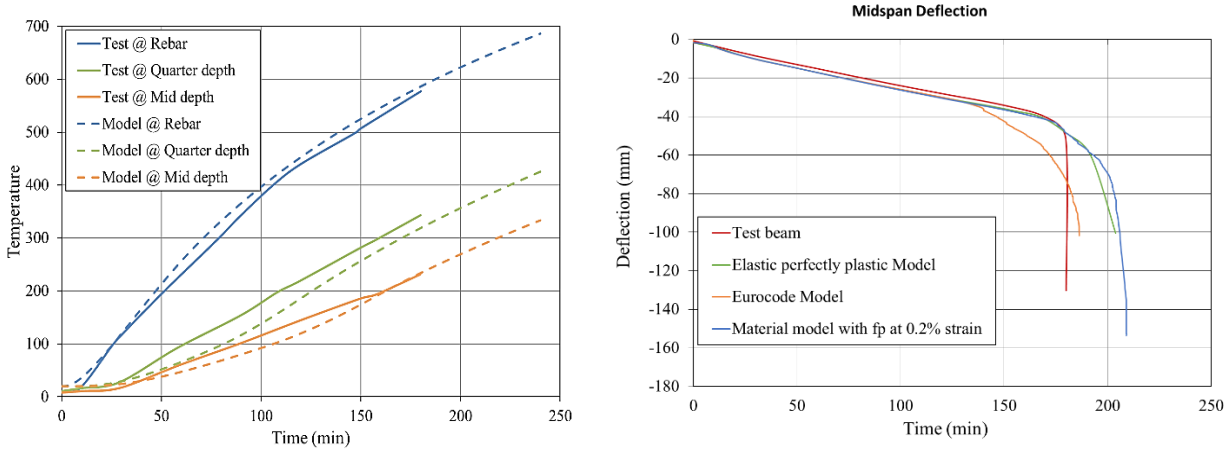

Figure 9: Comparison of predicted and measured rebar and concrete temperature and displacement for B-1.

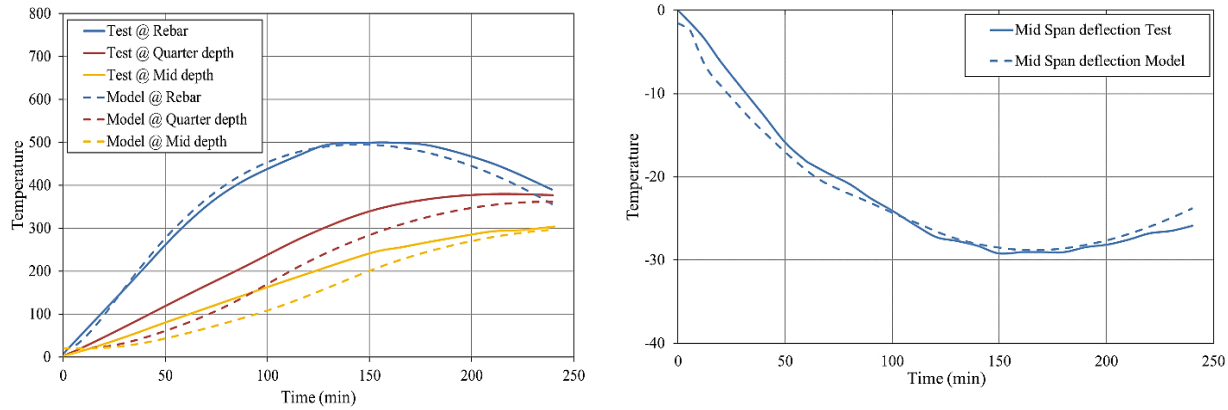

Figure 10. Comparison of predicted and measured rebar and concrete temperature and displacement for B-2.

Comparisons of results for the heat transfer model and structural analysis show that the two different assumptions made in this study, one for heat transfer analysis without radiation and the second for structural analysis with the proposed steel material model, work well with the test results.
The failure mode for B-1 is compression failure, whereas B-2 didn't fail due to short-term exposure to fire. The results are shown in figures (9) & (10) provide the comparison of the test beam and the numerical results.

5. Conclusion

A 3D FE model for predicting the behaviour of RC beams exposed to fire was discussed in this study. The heat transfer analysis without radiation and a new proportional limit for the steel material model is proposed in the current research, allowing for more accurate deflection predictions. The following conclusion can be drawn from this study.

- Heat transfer analysis in Abaqus [4] should be performed without taking the effect of radiation from surrounding fire unless a fire is modelled not in direct contact with RC beam.
- Elastic perfect plastic material model for steel rebar at elevated temperatures can be utilized in FEA. Strain hardening of steel at a given temperature can't be used due to the temperature rise during a fire.
- Plastic material model for steel rebar at elevated temperature can reduce the calculation time for the material model and a simulation time in Abaqus [4].
- New proposed proportional limit for steel rebar stress-strain curves at elevated temperature produces more accurate results.

References

1. J. Beitel and N. Iwankiw, "Analysis of Needs and Existing Capabilities for Full Scale Fire Resistance Testing" NIST GCR 02-843, 2002.
2. L. Taerwe, "From Member Design to Global Structural Behaviour" International workshop, Fire Design of Concrete Structures-From Materials Modelling to Structural Performance, University of Coimbra Portugal, November 2007.
3. N.N. Brushlinsky, M. Ahrens, S.V. Sokolov, and P. Wagner, "World fire statistics", CTIF, International Association of Fire and Rescue Services, No. 23, 2018.
   Available at: www.ctif.org/sites/default/files/ctif_report23_world_fire_statistics_2018_vs_2_0.pdf
4. 3DS/Simulia. ABAQUS/Standard: Abaqus Analysis User's Guide; 3DS/Dassault Systems, Providence, RI, USA, 2013.
5. W. Y. Gao, G. M. Chen , G. J. Teng, and J. G. Dai, 'Finite element modelling of reinforced concrete beams exposed to fire" Elsevier Ltd, 52, pp. 488–501, 2013. doi: 10.1016/j.engstruct.2013.03.017.
6. M. B. Dwaikat and V. K. R. Kodur, "Response of restrained concrete beams under design fire exposure", Journal of Structural Engineering, vol. 135, no. 11, pp. 1408–1417, 2009.
7. J. H. Liao, Z. D. Lu, and L. Su, "Experimental and finite element analysis of shear strength of concrete beams subjected to elevated temperature" Journal of Tongji University (Nature Science), 41(6), 806–812, 2013.
8. ISO 834-1, "Fire Resistance Tests-Elements of Building Construction. Part 1: General Requirement, International Organization for Standardization", Geneva, Switzerland, 1999.
9. ASTM E119, "Standard methods of fire test of building construction and materials. American society of testing and materials", West Conshohocken, PA, 2008.
10. Eurocode 2," Design of concrete structures Part 1-2: General rules - Structural fire design Euro code", SS-EN-1992-1-1:2008, 3 July 2004.
11. T.T. Lie, "Structural Fire Protection" American Society of Civil Engineers (ASCE) Manual and Reports on Engineering Practice No. 78.
12. P. Kmiecik, M. Kamiński, "Archives Of Civil And Mechanical Engineering". XI (3), 623,2011. http://dx.doi.org/10.1016/S1644-9665(12)60105-8
13. fib: Model Code for Concrete Structures 2010, Ernst and Son, 2013 (in press)
14. Wu, H. J.; Lie, T. T.; Hu, J. Y., "Fire Resistance of Beam-Slab Specimens: Experimental Studies" Internal Report (National Research Council of Canada. Institute for Research in Construction), no. IRC-IR-641, 1993-03.
15. Aliş, Betül, et al. "Investigation of Fire Effects on Reinforced Concrete Members via Finite Element Analysis." ACS Omega, vol. 7, no. 30, 2022, pp. 26881–26893., https://doi.org/10.1021/acsomega.2c03414.
16. Elshorbagy, Mohamed, and Mohamed Abdel-Mooty. "The Coupled Thermal-Structural Response of RC Beams during Fire Events Based on Nonlinear Numerical Simulation." Engineering Failure Analysis, vol. 109, 2020, p. 104297., https://doi.org/10.1016/j.engfailanal.2019.104297.